

Effect of heat treatment on structural and microstructural properties of $Mn_{0.5}Zn_{0.5}Fe_2O_4$ ferrite nanoparticles prepared by sol-gel auto combustion method

M. Deepty^{#a,b}, M. V. K. Mehar^{*c}, N. Krishna Mohan^{*d}

^aDepartment of Physics, Sasi Institute of Technology & Engineering, Tadepalligudem 534 101, India.

^bDepartment of Physics, Krishna University, Machilipatnam 521 001, India. ^cDepartment of Physics, Government Degree College, Alamuru 533 233, India.

^dDepartment of Physics, Akkineni Nageswara Rao Degree college, Guduwada, 521301, India.

*Corresponding authors: drmvkm@gmail.com, krishna_nutakki@yahoo.com

Abstract: Ferrite nanoparticles of $Mn_{0.5}Zn_{0.5}Fe_2O_4$ were successfully prepared by sol-gel auto combustion method. The ferrite nanoparticles are heat treated at different sintering temperatures of 600 °C, 750 °C and 900 °C in order to understand the influence of heat treatment on different physical properties. The lattice parameter and crystallite size were found to be increasing with the heat treatment. The nature of SEM reveals the agglomeration of ferrite fine particles into large clusters. The results are discussed in terms of cation redistribution and core-shell morphology.

Keywords: Ferrite nanoparticles; XRD; SEM; FTIR; Morphology.

I. INTRODUCTION

Synthesis and characterization of spinel ferrites possessing nanodimension crystallites have drawn much attention due to their versatile properties. The large surface to volume ratios is a prominent parameter in enhancing the magnetic, electrical, optical properties which can find potential applications in magnetic fluid, high density data storage, medical diagnostics, etc.[1]. Mn-Zn ferrite is one of the promising candidate which have been used in electronic applications, due to its high saturation magnetization, low eddy current losses, high permeability [2]. Mn-Zn ferrite is mixed ferrite of Mn-ferrite and Zn-ferrite. Mn occupies octahedral (B) sites and Zn occupies tetrahedral (A) sites in the spinel structure with the formula unit $(Zn^{2+}_{1-x}Fe^{3+}_x)[Mn^{2+}_xFe^{3+}_{2-x}]O_4$.

Spinel ferrites at nanoscale have been synthesized employing various chemical routes such as sol-gel [3], reverse micelle method [4], ultra sound irradiation [5], hydrothermal method, etc. [6]. Among all these methods co-precipitation method is highly preferable for preparation of ferrites because of easy preparation, composition flexibility, homogeneity, etc.

In the present study a series of $Mn_xZn_{1-x}Fe_2O_4$ ($x = 0.5, 0.6, 0.7$) ferrite nanoparticles have been synthesized using sol-gel auto combustion method and the samples were annealed at 600 °C, 750 °C and 900 °C. X-ray diffraction (XRD), scanning electron microscopy (SEM) and Fourier transform infrared spectroscopy (FTIR) have been employed for characterization. In the present paper the results of structural and FTIR analysis are reported.

II. EXPERIMENTAL PROCEDURE AND CHARACTERIZATION TECHNIQUES

A. PREPARATION:

$Mn_{0.5}Zn_{0.5}Fe_2O_4$ ferrite nanoparticles have been synthesized by sol-gel auto combustion technique. Analytical grade manganese sulfate ($MnSO_4 \cdot 7H_2O$), zinc sulfate ($ZnSO_4 \cdot 7H_2O$), ferric nitrate ($Fe(NO_3)_3 \cdot 9H_2O$) and citric acid ($C_6H_8O_7 \cdot H_2O$) are taken as precursors to prepare the present series of ferrite samples. The detailed procedure about the method synthesis was reported ever where [7].

B. CHARACTERIZATION TECHNIQUES:

The XRD patterns were recorded at room temperature using PANalytical X'pert-PRO powder diffractometer with CuK_α ($\lambda = 1.5406 \text{ \AA}$). The morphology of the samples was tested employing JEOL JSM-6610L scanning electron microscope. IR spectra for the ferrite samples were obtained in the range of 400 cm^{-1} to 4000 cm^{-1} with the help of Shimadzu IR-Prestige21 spectrometer.

III. RESULTS AND DISCUSSION

A. XRD Studies:

X-ray diffraction patterns obtained for the heat treated $Mn_{0.5}Zn_{0.5}Fe_2O_4$ ferrite samples at $600 \text{ }^\circ\text{C}$, $750 \text{ }^\circ\text{C}$ and $900 \text{ }^\circ\text{C}$ are presented in Fig.1. Powdered-X software is used to analyze the diffraction planes and the planes are indexed as (220), (311), (400), (422), (511) and (440). These are in good agreement with the earlier reports [8]. The broadening diffraction peaks is attributed to presence of ultrafine particles in the samples. The sharpness of the peaks is increasing with the heat treatment which indicates the improvement of crystallinity. The following relations have been used to structural and microstructural parameters. The average lattice constant values (a) were obtained using 2θ values of the most intense peaks using Bragg's diffraction condition given by

$$a = \frac{\lambda \sqrt{h^2 + k^2 + l^2}}{2 \sin \theta} \quad (1)$$

The average crystallite sizes are calculated with full width at half maximum of most intense peaks using Debye-Sherrer's equation given as

$$D = \frac{K \lambda}{\beta \cos \theta} \quad (2)$$

Where K is shape factor taken as 0.89, λ is the X-ray wavelength used and β is full width at half maximum intensity taking into account of instrumental broadening.

The X-ray density has been calculated using the relation

$$\rho_x = \frac{8M}{N_A a^3} \quad (3)$$

Where M is molecular weight of the ferrite sample, N_A is Avogadro's number and a is experimental lattice constant.

The lattice strain was estimated from the following derived relation modifying the Williamson and Hall equation

$$\eta = \frac{2d|K-1|}{D} \quad (4)$$

Where d is lattice spacing for (311) planes, D is the average crystallite size and K (0.89) is shape factor. The calculated values of lattice parameter (a), crystallite sizes (D), X-ray density (ρ_x) and lattice strain (η) are summarized in Table.1. The values of lattice parameter are in between the lattice parameters of $MnFe_2O_4$ (8.5706Å) and $ZnFe_2O_4$ (8.4475Å). It was observed that the lattice parameter monotonically increased with the heat treatment. This is attributed to the occupation of cations into their usual sites. The similar observations were reported even for other spinel ferrites also [9]. The crystallite sizes increases with the heat treatment and is related to Ostwald ripening, resulting the decrease of lattice strain. The variations in lattice parameter and crystallite size with the heat treatment is shown in Fig2. It was observed that the experimental density decreases with increase of sintering temperature. The variation of experimental density depends upon lattice parameter and molecular weight of ferrite. In the present study the variation of density depends on the variation of lattice parameter.

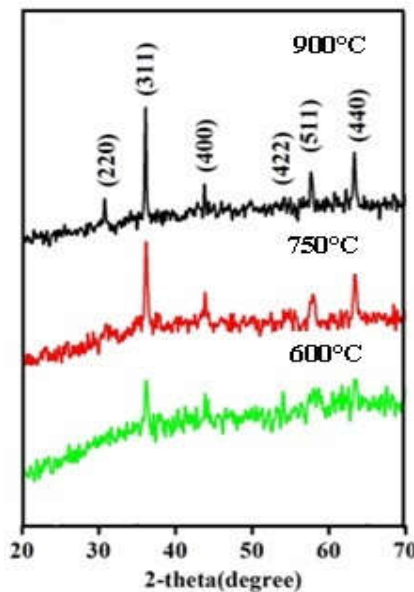


Fig.1 XRD Pattern of $Mn_{0.5}Zn_{0.5}Fe_2O_4$ heat treated at 600 °C, 750 °C and 900 °C

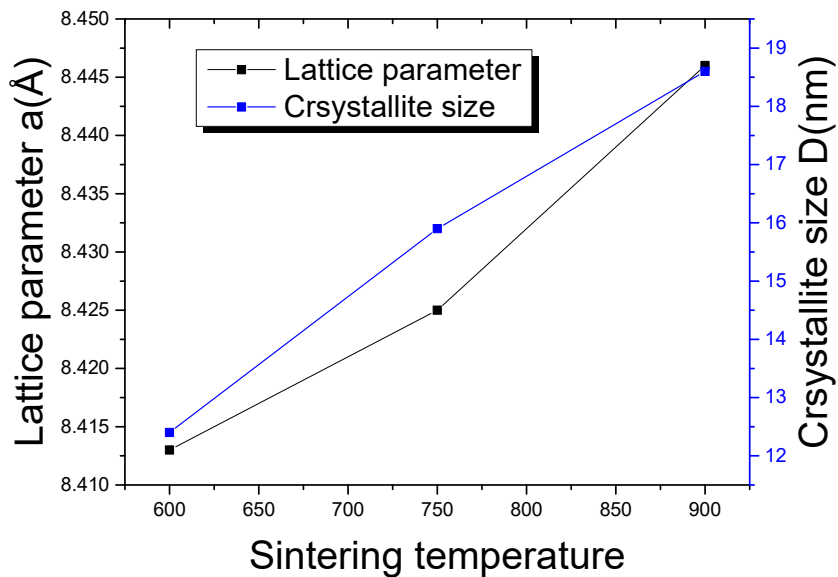


Fig.1 Plot of variation of D and a against to the heat treatment

TABLE 1

LATTICE PARAMETER (A), CRYSTALLITE SIZE (D), EXPERIMENTAL DENSITY (P_x) AND LATTICE STRAIN (H).

| Temp | $a(\text{\AA})$ | $D(\text{nm})$ | $\rho_x(\text{g/cm}^3)$ | $\eta (\times 10^{-3})$ |
|--------|-----------------|----------------|-------------------------|-------------------------|
| 600 °C | 8.413 | 12.4 | 4.875 | 6.65 |
| 750 °C | 8.425 | 15.9 | 4.813 | 5.56 |
| 900°C | 8.446 | 18.6 | 4.726 | 4.31 |

B.SEM STUDIES:

The SEM micrographs of annealed ferrite $\text{Mg}_{0.5}\text{Zn}_{0.5}\text{Fe}_2\text{O}_4$ at 600 °C, is shown in Fig. 3. The nature of SEM micrograph does not give any information about the ferrite nanoparticles. However, it reveals that the small sizes of ferrite nanoparticles are agglomerated into large clusters. Anwar et.al [10] reported the similar results for Cu substituted Mn-Zn nanoferrites. The close examination reveals the distribution of particles in different sizes which depends upon the nature of grain boundaries among the grains in the ferrite sample.

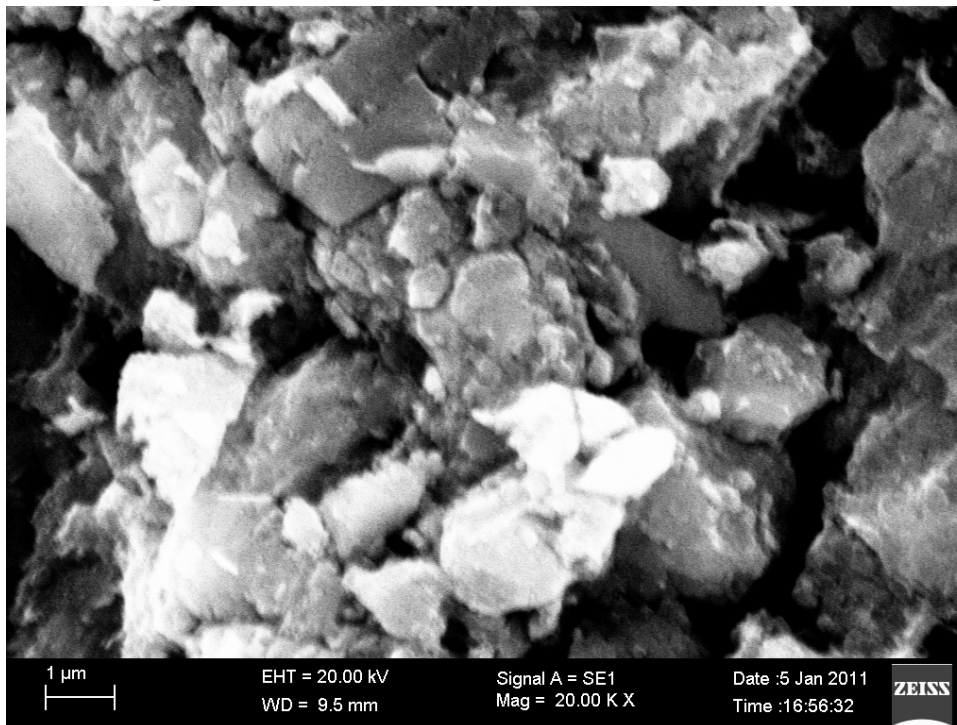


Fig.1 SEM micrograph of $\text{Mn}_{0.5}\text{Zn}_{0.5}\text{Fe}_2\text{O}_4$ heat treated at 600 °C

C.FTIR STUDIES:

Fourier Transform Infrared spectroscopy has been employed to observe the structural variations and spinel phase of ferrite systems. The two vibrational bands, one is higher vibrational frequency (ν_1) is in the range of $600\text{--}500\text{cm}^{-1}$ and the another one lower vibrational frequency (ν_2) is in the range $450\text{--}350\text{cm}^{-1}$ are the characteristic bands of cubic spinel structure [11]. The higher vibrational frequency (ν_1) is assigned to $\text{Fe}^{3+}\text{--O}^{2-}$ stretching vibrations at tetrahedral site (A) and the lower vibrational frequency (ν_2) is assigned to $\text{Fe}^{3+}\text{--O}^{2-}$ stretching vibrations at octahedral site (B). The FTIR spectra of heat treated $\text{Mn}_{0.5}\text{Zn}_{0.5}\text{Fe}_2\text{O}_4$ at 600 °C, 750 °C and 900 °C are shown in Fig.4. The tetrahedral and octahedral vibrational frequencies (ν_1 and ν_2) along with tetrahedral and octahedral force constants (K_T and K_O) are listed in Tab.2.

It was observed that the both tetrahedral and octahedral vibrational frequencies are shifted towards the lower frequencies with the heat treatment, which are ascribed to the elongation of $\text{Fe}^{3+} - \text{O}^{2-}$ bond lengths at both A and B sites. The variation of lattice force constants are in accordance with the variation of vibrational frequencies. The variation of vibrational frequencies supports the observed increase in lattice constant. M.A. Gabal et al [11] reported the increase in ν_1 and random variation in ν_2 . The increase in ν_1 and ν_2 in the present series is attributed to random distribution of cations in tetrahedral (A) and octahedral (B) sites against their normal preference. The peak near to 3500 cm^{-1} is ascribed to the presence of hydroxyl group retained in the sample during the preparation. This peak is disappeared at higher sintering temperatures due to evaporation of water.

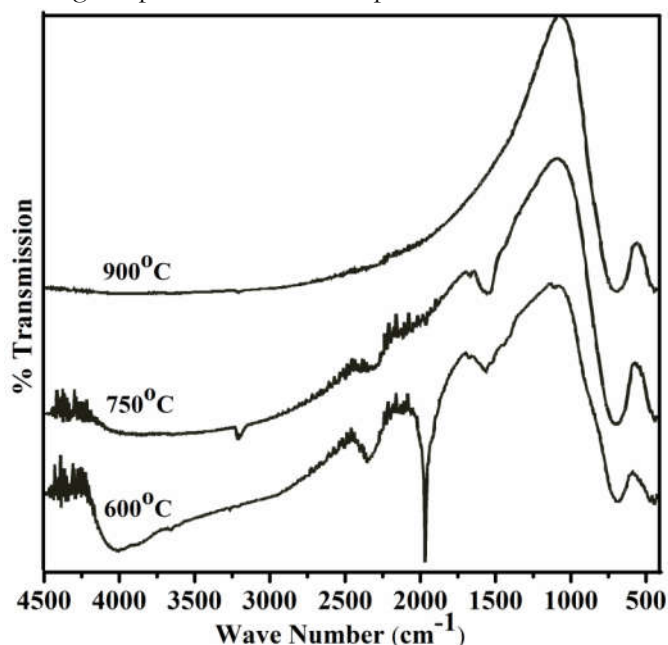


Fig.1 FTIR spectra of $\text{Mn}_{0.5}\text{Zn}_{0.5}\text{Fe}_2\text{O}_4$ heat treated at 600°C , 750°C and 900°C

TABLE 2

TETRAHEDRAL, OCTAHEDRAL VIBRATIONAL
FREQUENCIES (ν_1 AND ν_2) AND FORCE
CONSTANTS (K_T AND K_O)

| Temp | ν_1 (cm^{-1}) | ν_2 (cm^{-1}) | K_T | K_O |
|---------------------|------------------------------|------------------------------|----------------------------|----------------------------|
| | | | (dyne/cm) $\times 10^5$ | (dyne/cm) $\times 10^5$ |
| 600°C | 573.46 | 439.22 | 2.36 | 1.39 |
| 750°C | 571.21 | 435.06 | 2.21 | 1.32 |
| 900°C | 570.70 | 430.65 | 2.15 | 1.25 |

IV.CONCLUSION

Sol-gel auto combustion method is more suitable to prepare Mn-Zn ferrite to free from secondary phases. Sintering temperature is playing a crucial role on the structural and microstructural properties. The grain boundary energy is changing during the sintering process. This is a prominent factor to cause agglomeration of ferrite nanoparticles into the clusters. The present ferrite nanoparticles are the seems to be potential candidates for electromagnetic applications.

REFERENCES

1. R. C. Kambale, N. R. Adhate, B. K. Chougale, Y. D. Kolekar, *Magnetic and dielectric properties of mixed spinel Ni-Zn ferrites synthesized by citrate-nitrate combustion method*, *J. Alloy. Compd.* 49 (2010) 372-377.
2. A. Amirabadizadeh, H. Farsi, M. Dehghani, H. Arabi, *Effects of substitutions of Zn for Mn on size and magnetic properties of Mn-Zn ferrite nanoparticles*, *J. Supercond. Nov. Magn.* 25 (2012) 2763 – 2765.
3. Souilab Zabi, Mansor Hashim, A.R. Daud, *Synthesis, magnetic properties and microstructure of Ni-Zn ferrite by sol-gel technique*, *J. Magn. Mater.* 308 (2007) 177–182.
4. S. Gubbala, H. Nathani, K. Koizol, R. D. K. Misra, *Magnetic properties of nano-crystalline Ni-Zn, Zn-Mn and Ni-Mn ferrites synthesized by reverse micelle technique*, *Physica B* 348(2004)317–328.
5. Yasuaki Oohara, Jun Sugiyama, Masaaki Kontani, *Neutron scattering study of the charge ordering and spin ordering of the magnetically frustrated spinel antiferromagnet*, *J. Phys. Soc. Jpn.* 68(1999)242–246.
6. Jun Wang, Chuan Zeng, Zhenmeng Peng, Qianwang Chen, *Synthesis and magnetic properties of $Zn_{1-x}Mn_xFe_2O_4$ nanoparticles*, *Physica B* 349 (2004) 124–128.
7. M. Airimioaei, C.E. Ciomaga, N. Apostolescu, L. Leontie, A.R. Iordan, L. Mitoseriu, M. N. Palamaru, *Synthesis and functional properties of the $Ni_{1-x}Mn_xFe_2O_4$ ferrites*, *J. Alloy. Compd.* 509 (2011)8065–8072.
8. H. Mohseni, H. Shokrollahi, Ibrahim Sharifi, Kh. Gheisari, *Magnetic and structural studies of the Mn-doped Mg-Zn ferrite nanoparticles synthesized by the glycine nitrate process*, *J. Magn. Mater.* 324 (2012) 3741 – 3747.
9. Irshad Ali, M.U. Islam, M. Ishaque, Hasan M. Khan, Muhammad Naeem Ashiq, M.U. Rana, *Structural and magnetic properties of holmium substituted cobalt ferrites synthesized by chemical co-precipitation method*, *J. Magn. Mater.* 324 (2012) 3773–3777.
10. Humaira Anwar, Asghari Maqsood, *Structural, Magnetic and Electrical Properties of Cu Substituted Mn-Zn Soft Nanoferrites*, *J. Supercond. Nov. Magn* 25 (6) (2012)1913-1920.
11. R.D. Waldron, *Infrared spectra of ferrites*, *Phys. Rev.* 99(1955)1727–1735.
12. M. A. Gabal, S. Kosa, T. S. Al Mutairi, *Structural and magnetic properties of $Ni_{1-x}Zn_xFe_2O_4$ nano-crystalline ferrites prepared via novel chitosan method*, *J. Molec. Strut.* 1063 (2014) 269-273.